IMPROVING THE PERFORMANCE OF A GEOPHONE THROUGH CAPACITIVE POSITION SENSING AND FEEDBACK

Aaron Barzilai
Dept. of Mechanical Engineering
Stanford University
Stanford, CA

Tom VanZandt
Center for Space Microelectronics Technology
Jet Propulsion Laboratory
Pasadena, CA

Tom Kenny
Dept. of Mechanical Engineering
Stanford University
Stanford, CA

ABSTRACT

This paper reports on the improved performance of a geophone obtained by measuring the displacement of its proof mass capacitively rather than inductively and operating the sensor as a closed loop system. A measurement of the displacement of the proof mass rather than the velocity measurement made with a conventional geophone provides better low frequency performance. As a result, a geophone can be considered for use in a broader array of applications. A capacitive geophone can operate in either an open loop or closed loop mode. This paper describes a closed loop geophone system with a frequency response similar to the state of the art Streckeisen seismometers.

INTRODUCTION

Seismologists and geophysicists rely on a wide variety of sensors to study the Earth. Historically, a popular sensor in these communities has been the geophone, a highly sensitive ground motion transducer that have been in use for decades(Sheriff & Geldart, 1995). Figure 1 shows both a schematic drawing and a cross-sectional view of a geophone, which uses the motion of a spring supported coil in the field of a permanent magnet to generate an output signal. Studies of local and regional seismicity often rely on geophones. However, these sensors are most commonly used as sensors for seismic reflection and refraction surveys, techniques to image the three-dimensional structure of oil and gas deposits beneath the Earth's surface. For imaging applications, large, two-dimensional arrays of sensors are deployed on the surface to record seismic waves as they propagate below the ground. By measuring travel times and amplitudes of various components of the waves, the underground structures encountered by the waves can be determined.

The combination of attributes offered by a geophone make it a good choice for these applications and others. Riedesel et al.(1990) showed that a geophone can have a minimum instrumental noise as low as 0.1 $ng/\sqrt{Hz}$, which is quieter than the minimum seismic noise of the Earth(Peterson, 1993). The nominally 4.5 Hz GS-11D geophone by OYO Geospace used in this work has a minimum instrumental noise of 0.6 $ng/\sqrt{Hz}$(Barzilai

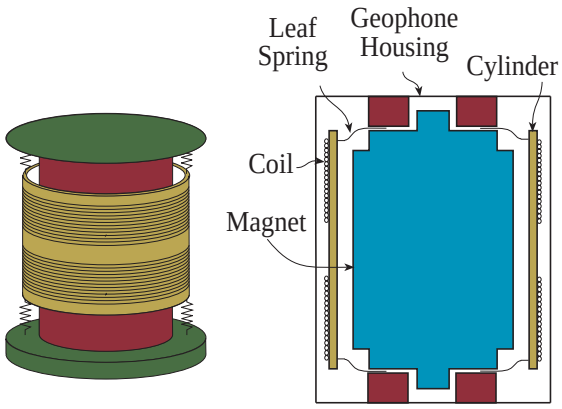

Figure 1: Schematic drawing and cross-sectional view of a geophone

et al. , 1998). The total harmonic distortion(THD) of a geophone is also quite low, less than 0.2% for the GS-11D. Geophones are also expected to be robust, capable of withstanding a one meter drop onto a piece of plywood 1000 times. Perhaps most importantly, geophones deliver this performance quite affordably, as one sensor costs on the order of $50 to $100.

However, a geophone is not an appropriate sensor for all applications. The noise of a geophone increases at frequencies below its resonance, making it a poor sensor for applications requiring low noise(10 ng), low frequency(1 mHz to 1 Hz) measurements. For these applications, such as studying seismic waves that have traveled great distances, a high end seismometer such as the Streckeisen line of seismometers would be more appropriate. The Streckeisen STS-2 has a constant sensitivity to ground velocity from 8.33 mHz to 50 Hz, with a resolution on the order of 0.01 $ng/\sqrt{Hz}$(Streckeisen AG, 1992). The STS-2 and other high performance seismometers sense their proof mass position capacitively rather than their proof mass velocity inductively as geophones do. Capacitive sensing enables better low frequency

performance than inductive sensing, since velocity is directly proportional to the frequency of the motion. Additionally, the STS-2 and others operate in a closed loop mode, enabling the manufacturer to modify the frequency response appropriately.

This improved performance of the STS-2 is accompanied by other drawbacks. High end seismometers can cost as much as $15,000 each. These seismometers are very fragile and much larger than a geophone. An STS-2 has a volume of 11,000 cm^3 and mass of 13 kg, while a GS-11D has a volume of 30 cm^3 and a mass of 140 g.

This paper reports on our efforts to modify a GS-11D to obtain a frequency response comparable to the STS-2 while maintaining the low cost of a geophone. This is accomplished by measuring the displacement of the geophone's proof mass capacitively and applying feedback to the geophone to control its response. Feedback seismometers have been widely discussed in the literature, with Usher et al.(1979) comparing the effects of displacement and velocity feedback. Klassen and Peppen(1983) built a closed loop geophone using velocity feedback. The motion of the coil was sensed inductively as a typical geophone does, and the feedback force was applied via a second coil inside the geophone. Their feedback geophone had a constant sensitivity to velocity from 0.5 Hz to 8 Hz. Since they used velocity feedback, Klassen and Peppen(1983) observed that like a conventional geophone, their closed loop geophone's noise was large at low frequencies.

The closed loop capacitive geophone has a few advantages over the approach of Klassen and Peppen (1983). The noise of the sensor at low frequencies is reduced by measuring the displacement of the proof mass rather than velocity. A commercial geophone is easily modified to make this capacitive measurement. Additionally, the closed loop capacitive geophone's constant sensitivity can be extended to higher frequencies.

GEOPHONE BACKGROUND

A geophone is a single axis seismometer that measures motion in the direction of its cylindrical axis. In typical near-surface deployments, a geophone is packaged with a conical spike and buried a few inches underground to ensure good coupling to the motion of the Earth. Ground motion causes the hollow cylinder of a geophone to move with respect to the geophone housing. The motion of this cylinder inside the geophone is described by Equation (1), the transfer function of a second-order mechanical system. Equation (1) expresses the relative position of the proof mass, X_r, for the acceleration applied to a geophone, $\ddot{X}_h$, as a function of frequency, with mass m[kg], spring constant k[N/m], and damping constant b[N/(m/s)].

$$\frac{X_r}{\ddot{X}_h} = \frac{-1}{s^2 + \frac{b}{m}s + \frac{k}{m}} \tag{1}$$

The cylinder's motion is measured by the interaction of the coil on the cylinder with the magnetic field of the permanent magnet inside the geophone. Faraday's Law, expressed in Equation (2) in the frequency domain, states that the voltage across a coil is equal to the change in flux through the coil with respect to time. In the case of a geophone, the change in flux through the coil versus coil displacement, $\partial\Phi/\partial x$, is constant for small displacements. Therefore, the voltage across the coil is directly proportional to the velocity of the coil. Geophone manufacturers typically report the constant of proportionality, G[V/(m/s) = N/A], known as the transduction constant or generator constant. Huan and Pater(1985) demonstrated that G varies by less than 0.05% as a function of position for displacements on the order of 10% of the maximum displacement.

$$V_0 = -\frac{\partial\Phi}{\partial t} = -\frac{\partial\Phi}{\partial x}\frac{\partial x}{\partial t} = -G\dot{X}_r = -GsX_r \tag{2}$$

The transfer function relating output voltage to input acceleration, given in Equation (3), can be determined by combining Equation (1) and Equation (2). The transfer function has been evaluated for the GS-11D used in this study. Unlike most accelerometers, this transfer function is not constant for signals at frequencies below the resonance, as shown in Figure 2. In Equation (3) and Figure 2, the transfer function has been evaluated for a conventional, nominally 4.5 Hz GS-11D geophone with the characteristics described in Table 1. To avoid this complicated frequency dependence of the sensitivity, seismologists consider the sensitivity of the output to velocity. As stated in Equation (4) and shown in Figure 3, the sensitivity of the output voltage to input velocity is constant at frequencies above the resonance. As a result, seismologists often express geophone outputs as velocity measurements and discard the information on signals with frequencies below the resonance(Dobrin, 1976). However, to enable comparisons with other accelerometers, this paper will express results in terms of accelerations. Seismologists often express their data in terms of both velocity and acceleration.

$$\frac{V_o}{\ddot{X}_h} = \frac{Gs}{s^2 + \frac{b}{m}s + \frac{k}{m}} = \frac{31.5s}{s^2 + 18s + 760} \tag{3}$$

$$\frac{V_o}{\dot{X}_h} = \frac{Gs^2}{s^2 + \frac{b}{m}s + \frac{k}{m}} = \frac{31.5s^2}{s^2 + 18s + 760} \tag{4}$$

The coil-magnetic field interaction inside a geophone that causes an output signal can also apply forces to the proof mass of the system. It is well known that the Lorentz force on a length of wire in the presence of a magnetic field is described by Equation (5), where B is the magnetic field, I is the current through the wire and l is the length of the wire. In the case of the geophone, the total force on the proof mass at low frequencies can be expressed more simply as the generator constant G multiplied by the current I[A], as shown in Equation (6).

$$F = i\mathbf{l} \times \mathbf{B} \tag{5}$$

$$F = GI \tag{6}$$

CAPACITIVE GEOPHONE

A conventional GS-11D was modified to enable capacitive measurement of the proof mass position. Figure 4 shows a cross-section of a capacitive geophone. Three holes are drilled into the case of the geophone, allowing access to the hollow cylinder that serves as the proof mass. An aluminum ring is then rigidly

Property	Conventional Geophone	Modified Geophone
Resonant Frequency	4.4 Hz	4.1 Hz
Damping Coefficient	.33	.30
Proof Mass	23 grams	26 grams
Sensitivity	32 V/(m/s)	32 V/(m/s)
DC Coil Resistance	380 Ω	380 Ω
Case to Coil Motion	1.8 mm	300 mm
Coil Inductance	50 mH	50 mH
Coil Parasitic Capacitance	50 pF	50 pF

Table 1: Properties of 4.5 Hz GS-11D geophone used in experiments

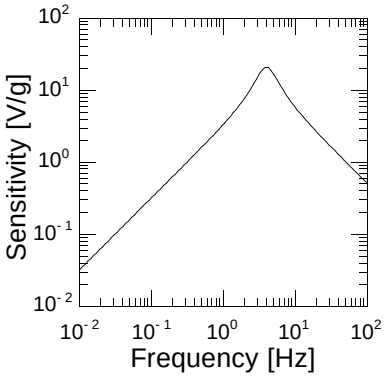

Figure 2: Predicted sensitivity of an OYO Geospace 4.5 Hz GS-11D geophone to acceleration

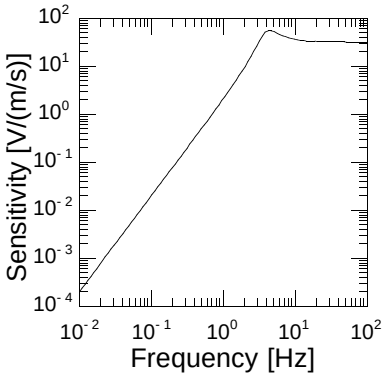

Figure 3: Predicted sensitivity of an OYO Geospace 4.5 Hz GS-11D geophone to velocity

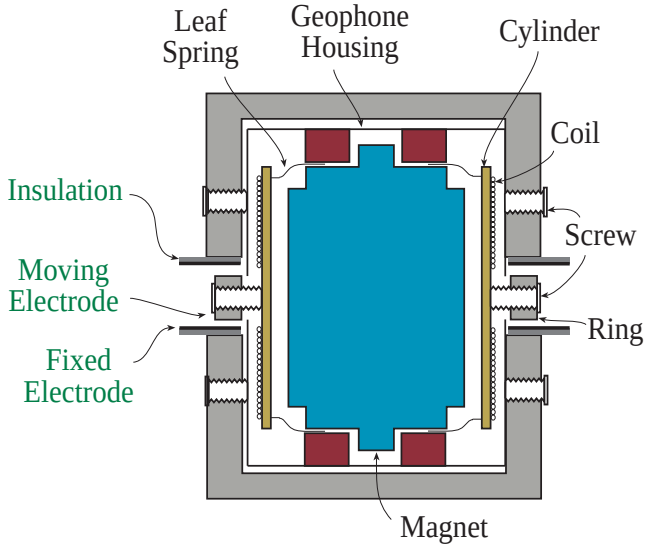

Figure 4: Cross-sectional view of a capacitive geophone(not to scale)

clamped to the cylinder by tightening the mounting screws. The ring has an outer diameter of 39.37 mm and an inner diameter of 33.37 mm. The height of the ring is 3.14 mm. The addition of 3 grams of mass to the nominal 23 grams of a conventional geophone changes the resonant frequency from 4.4 Hz to 4.1 Hz. Since the added mass is cylindrically symmetrical, no new twisting modes should be introduced by the hardware.

This ring serves as the moving center electrode of our capacitive sensor. The counter electrodes are two plates coated with copper on one side. These are rigidly attached to two aluminum cylinders, but no electrical connection is made. These two cylinders are then attached via set screws to the geophone housing. In this study, the fixed plates were mounted with a gap of roughly 3.75mm. Therefore, when the moving plate is centered, the gap between the moving electrode and each fixed electrode is 300 μm. The nominal capacitance in this case is 10 pF, assuming parallel plates. In practice, the hardware was manually assembled and is not completely aligned, but the plates are estimated to be within 3 degrees of parallel. Any misalignment will cause our output to deviate slightly from the predicted value.

The capacitance to voltage conversion circuit is shown in Figure 5. The circuit is based on the work of Burstein and Kaiser(1996). This approach was chosen because it linearizes the relation between capacitance and gap length, rejects spurious low frequency signals, and is easily implemented. Five volt square waves are applied to the fixed plates, 180 degrees out of phase. The voltage on the moving plate, V_{Br}, is then amplified by a non-inverting operational amplifier, which has a 10 MΩ resistor in parallel to dissipate op-amp input current. Equations (7) to (9) show how to solve for V_{Br}, where d[m] is the nominal gap between the fixed and moving electrodes, y[m] is the distance the center plate has moved from its nominal position, A[m^2] is the area of the capacitor plates, ϵ[] is the relative permittivity of air,

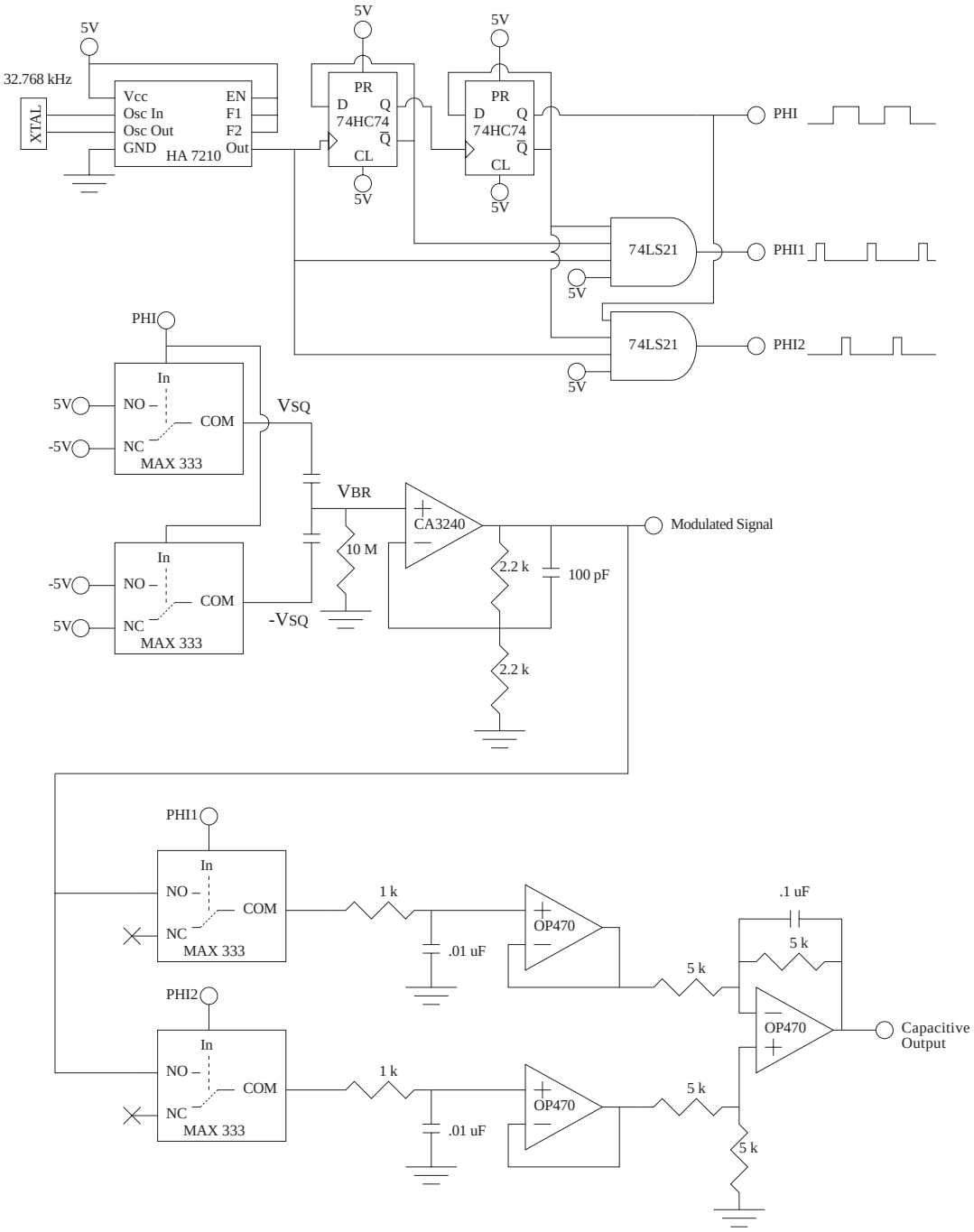

Figure 5: Circuit for capacitive position detection

and ϵ_0 [F/m] is the permittivity of free space, $8.85(10^{-12})$ F/m. Equation (9) shows that V_{Br} is a square wave whose amplitude is directly proportional to the motion of the center plate.

$$V_{Br} = ([V_{Sq} - (V_{Sq})]\frac{\frac{1}{sC_A}}{\frac{1}{sC_A} + \frac{1}{sC_B}}) - V_{Sq} = V_{Sq}\frac{s(C_B - C_A)}{s(C_B + C_A)} \quad (7)$$

$$V_{Sq}\frac{s(C_B - C_A)}{s(C_B + C_A)} = V_{Sq}\frac{\frac{\epsilon\epsilon_0 A}{d-y} - \frac{\epsilon\epsilon_0 A}{d+y}}{\frac{\epsilon\epsilon_0 A}{d-y} + \frac{\epsilon\epsilon_0 A}{d+y}} = V_{Sq}\frac{(d+y)-(d-y)}{(d+y)-(d-y)} \quad (8)$$

$$V_{Sq}\frac{(d+y)-(d-y)}{(d+y)-(d-y)} = V_{Sq}\frac{2y}{2d} = V_{Sq}\frac{y}{d} = V_{Br} \quad (9)$$

The demodulator circuit measures the modulated voltage during each half cycle of the square wave. This signal is sampled and low pass filtered with a 3 dB frequency of 15.9 kHz. Then, the difference between the half cycle voltages is found and low pass filtered with a 3 dB frequency of 318 Hz. The result is the amplitude of the square wave. This technique rejects DC or low frequency changes in V_{Br}, rejecting changes in the op-amp input current.

To verify our predicted relation, the capacitive geophone's proof mass was shaken and its motion measured capacitively and optically using a Polytec OFV3001 laser vibrometer. Figure 6 shows that the experimental result matches the prediction well at frequencies below 50 Hz, with a 10% larger signal than expected. At frequencies above 50 Hz, the experimentally obtained frequency response does not follow the prediction. This discrepancy becomes significant at frequencies close to 100 Hz, which should have little impact since it is outside the frequency range of interest, 8.33 mHz to 50 Hz. This experiment still enables the calibration of the voltage sensitivity to proof mass motion by examining lower frequencies.

In this experiment, a white noise force spectrum was applied, and the voltage spectrum of the capacitive output(not shown) matched the expected shape from DC to 300 Hz. Therefore, the discrepancy could indicate a higher order twisting mode which cannot be detected capacitively. Alternatively, errors in our data collection process could distort the vibrometer measurement at high frequency. If a higher order mode is present,

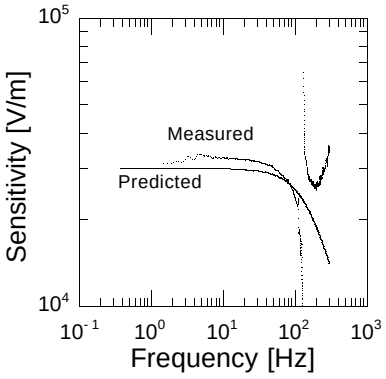

Figure 6: Predicted and measured sensitivity of capacitive position detection

it must be accounted for in the closed loop design.

The noise of a closed loop system can never be less than the noise of the sensor in the loop. It can be larger because of circuit noise introduced in the loop by other components, but sensor noise will never be attenuated by feedback. Therefore, the noise of the capacitive position measurement of the geophone is of great interest in both the open loop and closed loop case. To determine the open loop noise of the capacitive geophone, the output of the capacitive position measurement was monitored when two fixed reference capacitors replaced the capacitor plates of the geophone. This method was chosen since the instrumental noise will be much smaller than the seismic signals present in the laboratory, so we could not simply measure the position when no input was applied.

Figure 7 shows the noise of our capacitive measurement expressed as an equivalent acceleration input. It also shows the noise of a conventional GS-11D for reference(Barzilai *et al.* , 1998). As expected, capacitive measurement of acceleration has better resolution at lower frequencies, but the conventional geophone has better resolution at frequencies above 1 Hz. This will also be true for a closed loop capacitive geophone using this position sensing circuitry, since the noise of an open loop sensor sets a lower bound on the noise when that sensor is operated as a closed loop sensor.

CLOSED LOOP CAPACITIVE GEOPHONE

The capacitive geophone can be operated with feedback to tune the frequency response. The capacitive output provides a measure of the displacement of the proof mass. Restoring forces are applied by driving current through the coil. A block diagram of the system is shown in Figure 8.

A Bode plot of the open loop sensor's voltage vs. acceleration transfer function, appearing in Figure 9, shows that the magnitude crosses 1 at 20 Hz, but with little phase margin. To push the crossover frequency above 50 Hz and obtain more damping, a double lead controller was implemented with lag present to provide high gain at DC. A simple lead controller would not provide enough lead to obtain a reasonable amount of damping,

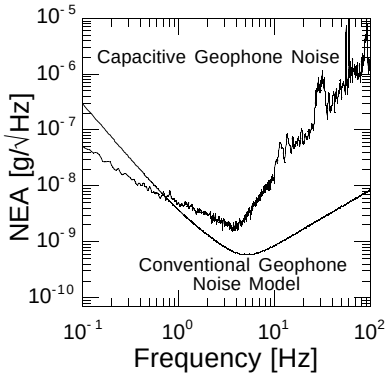

Figure 7: Measured noise equivalent acceleration(NEA) of a capacitive GS-11D geophone and predicted NEA of a conventional GS-11D

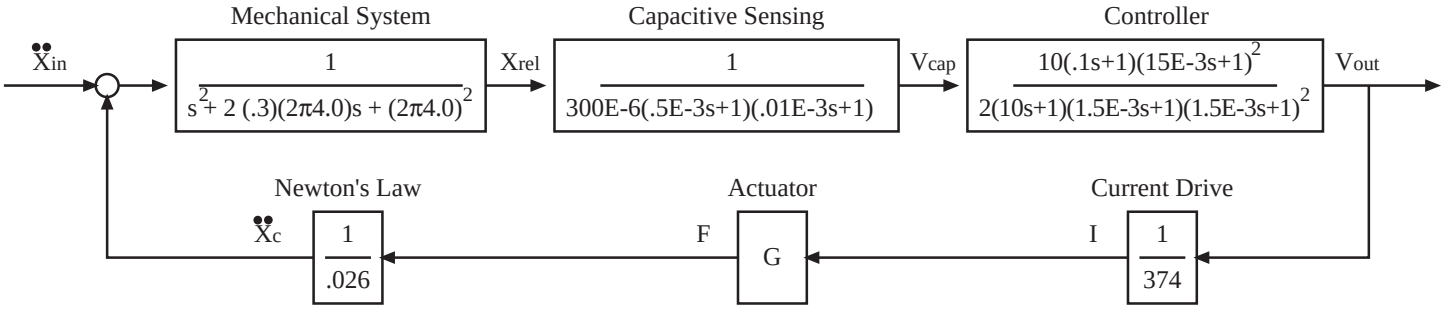

Figure 8: Block diagram of closed loop capacitive geophone system

so a second lead circuit was placed in series to double the lead added by the controller. The lag portion of the controller was necessary to provide high gain at DC. This ensures that feedback causes the geophone to center the moving electrode regardless of the effect of the gravitational field, which might vary due to sensor tilt. Figure 10 shows the Bode plot of this controller.

The loop gain of the closed loop system is plotted in Figure 11. The magnitude becomes less than one at 40 to 45 Hz, with a phase margin of 65 degrees, indicating that the closed loop response will be adequately damped. The predicted and measured closed loop sensitivity is shown in Figure 12. The measured sensitivity was determined by comparing the closed loop capacitive geophone to a reference sensor. The low frequency data was gathered with an EG&G IC Sensors 3145 accelerometer. This data matches the prediction very well. For the high frequency data, a conventional geophone was used as a reference. This data indicates that the bandwidth prediction is very good, but the scale factor is off by 10%. The measured data is inconclusive in indicating that no other modes of oscillation play a significant role in determining the frequency response the geophone has been improved over the decades to reduce spurious resonances, so any present probably result from the mechanical system added to the geophone.

Closing the loop offers many benefits to the capacitive geophone. Attenuating the motion of the proof mass for a fixed input improves both dynamic range and linearity. Figure 13 shows motion has been reduced by as much two orders of magnitude or more at low frequencies. Dynamic range should be improved by reducing the motion, since the closed loop noise should match the open loop noise magnitudes, while the closed loop systems can respond to larger signals without clipping. Linearity should be improved because non-linearities in the spring of the geophone can be significant. Reduced proof mass motion lessens the effect this non-linearity can have. The capacitive sensing should not introduce non-linearity, because the circuitry is arranged to provide an output that is linear with respect to proof mass motion.

CONCLUSIONS AND FUTURE WORK

The performance of a geophone has been enhanced by measuring the position of its proof mass capacitively and operating the sensor in a closed loop mode. The most important benefits of these changes are improved low frequency noise and wider bandwidth. With these simple modifications, a geophone can

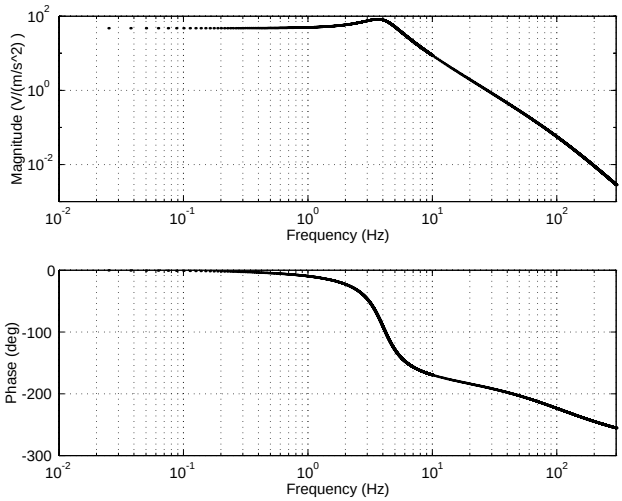

Figure 9: Predicted capacitive geophone open loop frequency response

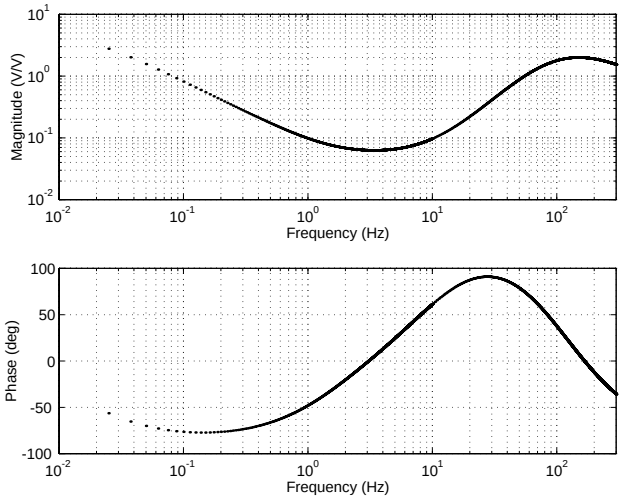

Figure 10: Predicted open loop frequency response of closed loop geophone controller

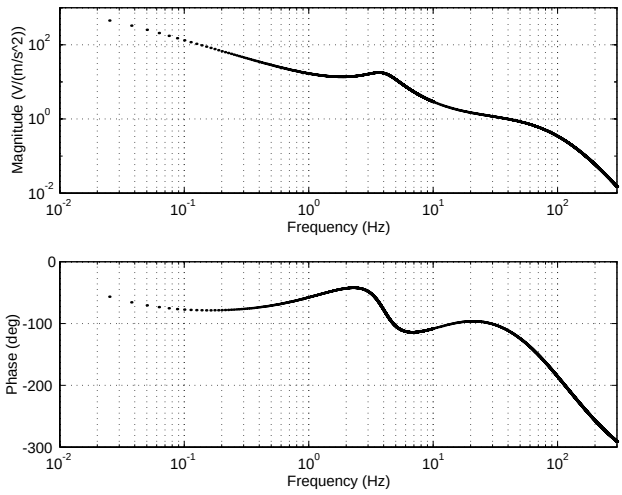

Figure 11: Predicted loop gain of closed loop geophone controller

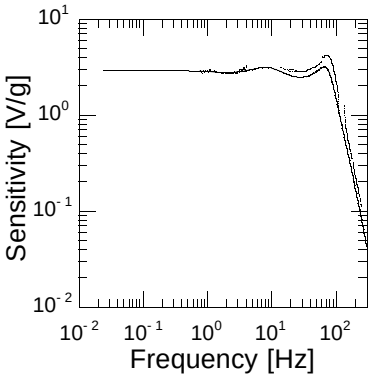

Figure 12: Predicted(-) and measured(.) sensitivity of a closed loop capacitive geophone

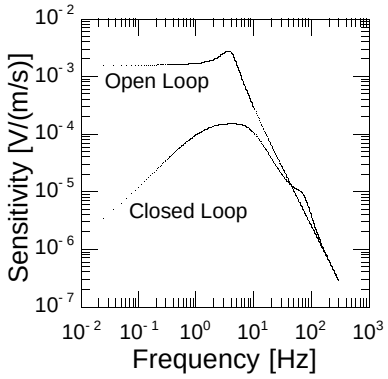

Figure 13: Predicted transfer function between geophone proof mass and input acceleration when operated as an open loop and closed loop sensor

offer performance rivalling that of high performance seismometers for a fraction of the cost, perhaps $500-$1000 vs. a $15,000 STS-2. These changes will modestly increase the size of a geophone and should not significantly reduce the robustness of the instrument as the mechanical resonant frequency has not been reduced significantly.

This approach for improving geophones can be further refined. Improved controllers that provide a flatter closed loop frequency response should be implemented. In the future, the low frequency performance will be fully characterized, studying noise and frequency response at much lower frequencies. Other circuit architectures should be investigated to reduce the low frequency noise further. Of course, high performance seismometers have important specifications besides noise and frequency response. Temperature coefficients, linearity, and dynamic range are all crucial aspects of a seismometer. In addition to improvements in the capacitive geophone's noise and frequency response, these parameters must also be characterized and improved if necessary.

ACKNOWLEDGMENTS

This work was supported by the Center for Space Microelectronics Technology, Jet Propulsion Laboratory, California Institute of Technology, and is sponsored by the National Aeronautics and Space Administration, Office of Space Access and Technology. We also acknowledge the National Science Foundation CAREER Award (ECS-9502046), the Charles Lee Powell Foundation, and the Terman Fellowship.

REFERENCES

Barzilai, A., VanZandt, T., & Kenny, T. 1998. Technique for measurement of the noise of a sensor in the presence of large background signals. *Review of Scientific Instruments*, **Accepted For Publication**.

Burstein, A., & Kaiser, W. J. 1996. Mixed analog-digital highly sensitive sensor interface circuit for low-cost microsensors. *Sensors and Actuators A*, **52**, 193–197.

Dobrin, M. B. 1976. *Introduction to Geophysical Prospecting*. Third edn. New York: McGraw-Hill.

Huan, S. L., & Pater, A. R. 1985. Analysis and prediction of geophone performance parameters. *Geophysics*, **50**(8), 1221–1228.

Klassen, K. B., & Van Peppen, J. C. L. 1983. Electronic Acceleration-Sensitive Geophone For Seismic Prospecting. *Geophysical Prospecting*, **31**, 457–480.

Peterson, J. 1993. *Observations and Modeling of Seismic Background Noise*. Tech. rept. 93-322. United States Geological Society Open-File Report.

Riedesel, M., Moore, R. D., & Orcutt, J. A. 1990. Limits of Sensitivity of Seismometers with Velocity Transducers and Electronic Amplifiers. *Bulletin of the Seismological Society of America*, **80**(6), 1725–1752.

Sheriff, R. E., & Geldart, L. P. 1995. *Exploration Seismology*. Second edn. New York: Cambridge University Press.

Streckeisen AG. 1992. *STS-2 Manual*. Pfungen, Switzerland.

Usher, M.J., Burch, R. F., & Guralp, C. 1979. Wideband Feedback Seismometers. *Physics of the Earth and Planetary Interiors*, **18**, 38–50.